

VTON-HandFit: Virtual Try-on for Arbitrary Hand Pose Guided by Hand Priors Embedding

Yujie Liang^{1*}, Xiaobin Hu^{2*}, Boyuan Jiang², Donghao Luo^{2†}, Kai Wu²,
Wenhui Han², Taisong Jin^{1†}, Chengjie Wang²

¹Xiamen University, ²Tencent

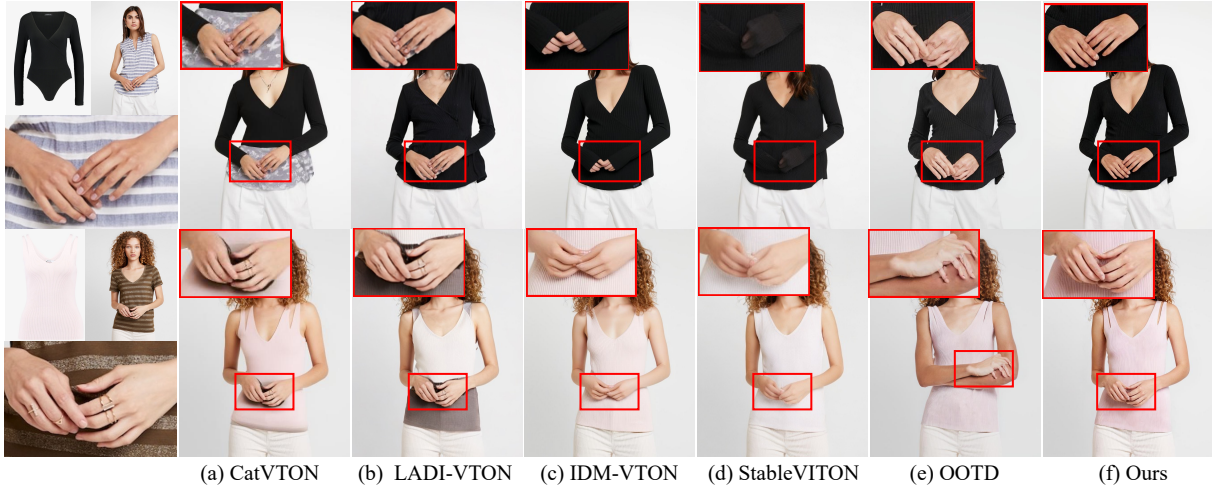


Figure 1: Comparison of different models on virtual try-on with hand occlusion. The leftmost three images are reference images from the VITON-HD test set, showing the target clothing, the model, and a close-up of the model’s hand. Our model excels in preserving hand details and achieving realistic clothing transfer, as highlighted in the red boxes. CatVTON and LADI-VTON utilize a parsing model to retain the hand segment, resulting in the inevitable persistence of residual artifacts and backgrounds from the model image.

Abstract

Although diffusion-based image virtual try-on has made considerable progress, emerging approaches still struggle to effectively address the issue of hand occlusion (*i.e.*, clothing regions occluded by the hand part), leading to a notable degradation of the try-on performance. To tackle this issue widely existing in real-world scenarios, we propose VTON-HandFit, leveraging the power of hand priors to reconstruct the appearance and structure for hand occlusion cases. Firstly, we tailor a *Handpose Aggregation Net* using the ControlNet-based structure explicitly and adaptively encoding the global hand and pose priors. Besides, to fully exploit the hand-related structure and appearance information, we propose *Hand-feature Disentanglement Embedding* module to disentangle the hand priors into the hand structure-parametric and visual-appearance features, and customize a masked cross attention for further decoupled feature embedding. Lastly, we customize a hand-canny constraint loss to better learn the structure edge knowledge from the hand template of model image. VTON-HandFit outperforms the baselines in qualitative and quantitative evaluations on the public dataset and

our self-collected hand-occlusion Handfit-3K dataset particularly for the arbitrary hand pose occlusion cases in real-world scenarios. The code and dataset will be available at <https://github.com/VTON-HandFit/VTON-HandFit>.

Introduction

Image-based virtual try-on (VTON) (Lee et al. 2022) is a widely adopted and highly promising image synthesis technology in the e-commerce industry. Its primary goal is to enhance the shopping experience for consumers and minimize advertising expenses for clothing merchants. The VTON task involves generating an image of a human model wearing a specific garment. Over the past few years, countless researchers (Yang et al. 2020; Dong et al. 2019; Ge et al. 2021a; Davide et al. 2022) have dedicated significant efforts to achieve more realistic and precise virtual try-on results.

Most recent studies on virtual try-on predominantly utilize generative adversarial networks (GANs) (Goodfellow et al. 2020) or latent diffusion models (LDMs) (Rombach et al. 2022) for image synthesis. However, traditional GAN-based approaches (Han et al. 2019, 2018; He, Song, and Xiang 2022) often struggle with accurately generating gar-

*Equal contributions.

†Corresponding authors.

ment folds, realistic lighting and shadows, and lifelike human body representations. Consequently, more recent research has shifted towards LDM-based methods (Zhu et al. 2023), which effectively improve the authenticity of clothed images. However, these researches focus on generating more realistic and natural try-on images while keeping the detailed features of garments. The hands of try-on models are usually strictly on the sides and garments are not occluded by the hands. Such a strict constraint hinders the virtual try-on paving the way toward real-world applications. For instance, as a highly flexible editing task with a wide range of degrees of freedom, digital humans usually meet the occasions that the garments are occluded by the hands, which severely deteriorates the performance of virtual try-on.

Motivated by the above challenge, basically, there mainly exist two solutions to tackle this arbitrary hand problem: 1). perfect hand parsing model to accurately segment the tiny area among fingers. 2). involving the hand-reconstruction into the try-on processing. As shown in Fig. 1, CatVTON and LADI-VTON use the parsing model to keep the hand part, leading to unavoidably the remaining artifacts and backgrounds from the model image. The existing parsing models fail to accurately segment the small and fragmented finger areas, thus we embrace the latter strategy to involve the hand-reconstruction by disentangling the hand into the appearance and structure knowledge processing in the try-on stage. Then, we propose a novel diffusion-based virtual try-on method, termed as VTON-HandFit, to generate realistic and natural images for arbitrary hand position or hand-occlusion cases with the aid of hand 3D structure-parametric and visual-appearance priors. To embed the pose and hand-related knowledge, we build a Handpose-Net to exploit the body and hand semantic and structure information by getting the body (*e.g.*, DWPose, DensPose) and 3D hand HaMeR-based (Zhu et al. 2023) reconstruction information. Secondly, considering the over-small character of hand that is easily ignored after down-sampling operation, we use the DINO (Zhang et al. 2023) to dig the local appearance and texture knowledge of hand as the hand-visual embedding features. For the structure of hand, we adopt these structure-parametric priors (*e.g.*, 3D MANO-related parameters, handtype and hand-box coordinates) as hand-structure embedding features. After getting structure-parametric and visual-appearance features, we aim to enhance the model’s ability to respectively learn hand-related patterns. To achieve this, we inject the hand-structure embedding into the HandPose-Net with a primary focus on enhancing the latent features related to hand structure, and the hand-visual embedding into the mainstream U-Net specifically aiming to enhance texture-related features, respectively. The disentanglement learning of structure and visual appearance enhances the network’s ability to efficiently and respectively acquire hand-related knowledge. To prevent the interference of hand-related priors with garment features, we impose a constraint that restricts the hand-related features to operate solely within the hand mask area of the cross-attention mechanism. Finally, we tailor a hand-canny constraint loss to more effectively acquire the structural edge knowledge from the hand template of the model image. Our

contributions are summarized as follows:

- We propose VTON-HandFit, a novel virtual try-on architecture considering to solve the Hand pose occlusion problem popularly existing in real-world scenarios.
- We propose a Hand-Pose Aggregation Net to encode the hand and pose structure priors and also adaptively to adjust the weight of each component. Meanwhile, hand-canny constraint loss is designed to learn the hand structural-edge knowledge of model images.
- We propose a novel hand-feature disentanglement embedding module disentangling the hand knowledge into the structure-parametric priors (*e.g.*, MANO parameters) and visual-appearance priors (*e.g.*, color). A mask cross-attention mechanism is proposed to constrain the hand-related features only working on the hand mask area to avoid the garment feature disturbance.
- We self-collect Handfit-3K test dataset from online retail sites to evaluate hand occlusion performance. Extensive qualitative and quantitative evaluations demonstrate our superiority over state-of-the-art virtual try-on models especially for hand pose occlusion cases, paving the road towards more complicated virtual try-on in real-world.

Related Works

Image-based virtual try-on. In the context of image-based virtual try-on, the objective is to generate a realistic representation of a target person wearing a specific garment, given a pair of corresponding images. A series of studies (Lee et al. 2022; Men et al. 2020; Xie et al. 2023; Yang et al. 2023b) have been conducted using Generative Adversarial Networks (GANs) (Goodfellow et al. 2020). These studies typically involve the initial deformation of the garment to match the body shape of the person, followed by the utilization of a generator to superimpose the deformed garment onto the person image. Despite efforts made to minimize the discrepancy between the warped garment and the person (Ge et al. 2021b; Issenhuth, Mary, and Calauzenes 2020; Lee et al. 2022), these approaches often lack the ability to generalize well to diverse person images, particularly those with complex backgrounds or intricate poses. There exists GAN-based try-on method (Lee et al. 2022) considers occluded problems and designs the warping operation to avoid the garment warping misalignment, which is totally different from diffusion-based algorithms as an inpainting problem.

The remarkable generative capabilities of diffusion models have sparked interest in incorporating them into fashion synthesis, particularly in tasks like visual try-on (Bhunja et al. 2023; Cao et al. 2023; Karras et al. 2023; Chen et al. 2024; Li et al. 2024; Zhang et al. 2024; Sun et al. 2024). TryOnDiffusion (Zhu et al. 2023) employs Parallel-UNets to preserve garment details and warp the garment for the try-on process. Subsequent studies have treated virtual try-on as an exemplar-based image inpainting problem (Yang et al. 2023a). These studies involved fine-tuning the inpainting diffusion models using virtual try-on datasets (Kim et al. 2024; Morelli et al. 2023) to generate virtual try-on images of superior quality. For instance, such as LADI-VTON (Morelli et al. 2023) and DCI-VTON (Gou et al. 2023) have emerged, treating clothing as pseudo-words or employ-

ing warping networks to integrate garments into pre-trained diffusion models. IDM-VTON (Choi et al. 2024) incorporates sophisticated attention modules to encode the high-level semantics of the garment and extract low-level features, thereby preserving fine-grained details. While these diffusion methods address issues related to the nature and realism of synthesized images, they struggle to meet hard occasions of the hand-based occlusion which very widely exists in the real-world virtual try-on scenarios.

Conditional control of diffusion models. In recent years, latent diffusion models (Rombach et al. 2022) have demonstrated significant success in tasks such as text-to-image generation (Ruiz et al. 2023; Kumari et al. 2023; Podell et al. 2023; Hu et al. 2024) and image-to-image generation (Kawar et al. 2023; Saharia et al. 2022). To achieve more controllable generated results, several studies have introduced conditional control to diffusion models (Ye et al. 2023; Zhao et al. 2024). ControlNet (Zhang, Rao, and Agrawala 2023) adds spatial conditioning controls (*e.g.*,anny edges, Hough lines, user scribbles, human key points) to pretrained diffusion models via zero convolutions manner. T2I-Adapter (Mou et al. 2024) aligns the internal knowledge within T2I models with external control signals, allowing it to be trained based on different conditions. This approach enables the generation of results with rich control and editing effects, particularly in terms of color and structure. In our paper, we focus on the hard occasions of hand-based occlusion in image-based VTON task, and tailor a Hand-Pose Aggregation Net to control the body pose and hand structure. Furthermore, the disengagement knowledge of hand structure and appearance embedding is studied and then these embeddings are respectively injected into the attention mechanism, acting as a mask-based regional control.

Reliable human hand generation. Previous studies (Samuel et al. 2024) have acknowledged the problem of misshaped hands that are generated by existing text-to-image diffusion models. Controlling the hand is considerably more challenging compared to controlling the body pose, primarily due to the relative size of the main subject. Besides, diffusion models exhibit significantly improved capability in generating plausible whole-body poses. This difficulty arises from the intricate nature of learning the physical structure and pose of hands from training images, which encompasses extensive deformations and occlusions. Handrefiner (Lu et al. 2023) and RHandS (Wang et al. 2024) are post-processing solutions adopting a hand mesh reconstruction model to rectify malformed hands. VTON-HandFit involves the hand corrections into the generation process not as a post-processing and disentangles the hand priors into the structure and appearance feature embedding for virtual try-on arbitrary hand pose in the real-world.

Methodology

Data collection of Handfit-3K. Considering that the hand of the current main virtual try-on dataset is separate from the body, there rarely exists a great amount of virtual try-on data for arbitrary hand pose and hard hand-occlusion cases. To meet this urgent need in real-world, we aim to construct a dataset of complex hand poses that occlude the garment.

Specifically, we collect an additional dataset of 26,000 images sourced from online retail sites. These images underwent processing using a parsing model and a hand bounding box via HaMeR model (Pavlakos et al. 2024) to identify instances of occlusion. We devote significant manual effort to inspecting the quality of the data, removing any erroneous or flawed entries, thereby ensuring the high quality of the virtual try-on dataset. As a result, we obtained a specialized hand occlusion test set comprising 3,620 images, termed as Handfit-3K. This dataset facilitates a targeted evaluation of our method’s ability to effectively handle occlusions.

Preliminary

Latent Diffusion Models. Our VTON-HandFit is an extension of stable diffusion model, which is a probabilistic model specifically designed to estimate a data distribution $p(x)$ by iteratively reducing noise in a normally distributed variable. Given an input image x_0 , the noise estimation process is:

$$\mathcal{L}_{noise} = \mathbb{E}_{z \sim \mathcal{E}(x), C, \epsilon \sim \mathcal{N}(0,1), t} [\|\epsilon - \epsilon_\theta(z_t, t, C)\|_2^2], \quad (1)$$

where a Variational AutoEncoder \mathcal{E} compress input image x into low-dimension latent space z . A conditional U-Net denoiser ϵ_θ aims to estimate noise θ in latent space with the aid of timestep t , t -th noisy latent representation z_t , and other text-prompt conditions C extracted by text-encoder.

VTON-HandFit

Overview. An overview of our VTON-HandFit is illustrated in Fig. 2. Given a target person image $x \in \mathbb{R}^{H \times W \times 3}$ and an input garment image $g \in \mathbb{R}^{H \times W \times 3}$, VTON-HandFit aims to generate a realistic outfitted image $x_g \in \mathbb{R}^{H \times W \times 3}$. The garment-agnostic person representation x_m is masked to erase the garment information by the combination of HumanParsing and HumanPose. Thus, this virtual try-on task is transformed into an example-based inpainting problem to recover the missing mask part. For the input of TryonNet, we simply concatenate the noise image (z_t) and latent garment-agnostic features $\mathcal{E}(x_m)$ to avoid the other pose-relevant information disturbances. In Hand-Pose Aggregation Net, we also aggregate the pose-related knowledge including the DWPose, DensePose and 3D reconstruction depth map derived by the HaMeR mesh model. These pose-related priors are detached with TryonNet to explicitly be learned in Hand-Pose Net. DensePose provides more body-semantic information, DWPose contains abundant skeleton structure, and 3D-hand-derived depth maps demonstrate the pixel-level global-aligned hand position and structure knowledge. These modules complement each other by mutually providing information, and working together to constrain the pose and hand generation. In hand-feature disentanglement embedding, we use the HaMeR model for 3D hand reconstruction and get the structure-parametric priors. These features are processed by the Hand-Struct processor to derive structural features c_{struct} . Simultaneously, cropped hand images are processed by DINOv2 and the Hand-Appear processor to obtain visual features c_{appear} . Besides, GarmentNet aims to extract the garment features into the TryonNet mainly by: 1). encoding the garment image into the latent space \mathcal{E}_g , 2). using the CLIP to get the image token features for injection. **Hand-Pose Aggregation Net.** To aggregate the hand and pose-relevant priors learning, we tailor a HandposeNet to

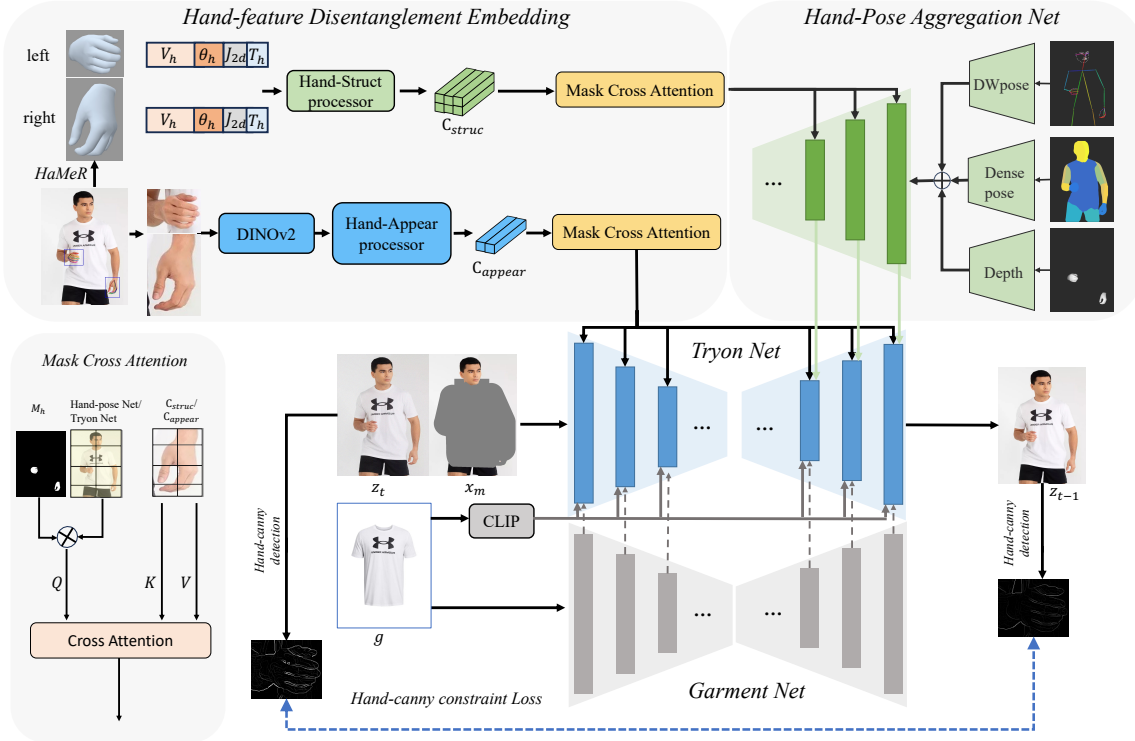


Figure 2: An overview of our VTON-HandFit Network. The network consists of two main components: Hand-feature Disentanglement Embedding and Hand-Pose Aggregation Net. The Hand-feature Disentanglement Embedding module uses the HaMeR model to extract hand priors, including hand type T_h , 3D vertices V_h , spatial joint locations J_{2d} , and joint rotation matrices θ_h . These features are processed by the Hand-Struct processor to derive structural features C_{struc} . Simultaneously, hand images cropped using bounding boxes are processed by DINOv2 and the Hand-Appear processor to obtain visual features C_{appear} . The structural and visual features are integrated using mask cross attention. The Hand-Pose Aggregation Net module controls body and hand poses by aggregating DWpose, Densepose, and hand depth maps.

constrain the semantic and skeleton pose, and global pixel-level hand knowledge. Specifically, $dwpose$, $densepose$, and $render$ blocks are designed based on the same zero-multilayer structure with different weights to respectively extract the corresponding features. Zero-multilayer structure consists of seven stacking of $conv$ and SiLU activate function with the zero convolution layer at the last layer.

$$\mathcal{F}_{hp} = \mathcal{F}_{dw} + \mathcal{F}_{dp} + \mathcal{F}_{rh} \times w_{hand}, \quad (2)$$

where \mathcal{F}_{dw} , \mathcal{F}_{dp} , \mathcal{F}_{rh} are the DWPose feature, Densepose feature, and hand feature after the Zero-multilayer structure, and then the summation is implemented on the pixel-level with the adjustable weight w_{hand} of hand feature \mathcal{F}_{rh} . To mitigate the impact of detrimental noise on the hidden states of the neural network layers in the trainable HandposeNet during the initial stages of training, we also adopt the zero convolution learning paradigm of ControlNet.

Hand structural embedding. The HaMeR (Pavlakos et al. 2024) model is utilized to reconstruct various MANO parameters and other hand-related information from 2D images, including hand mask $M_h \in \mathbb{R}^{n \times 768 \times 1024}$, hand types $T_h \in \mathbb{R}^{n \times 1}$, hand 3D vertices $V_h \in \mathbb{R}^{n \times 778 \times 3}$, spatial joint locations $J_{2d} \in \mathbb{R}^{n \times 21 \times 2}$, and joint rotation matrices $\theta \in \mathbb{R}^{n \times 16 \times 3 \times 3}$ where n represents the number of hands. To accommodate variable numbers of hands as input, we pad the hand parameters to a fixed length $n = 2$ by adding padding at the end. For hand type T_h , we use 0 to denote left hands, 1 for right hands, and -1 as a filler for images

without hands. Similar padding is applied to other parameters to ensure alignment and correspondence across all dimensions. We apply Basis Point Set (BPS) (Prokudin, Lassner, and Romero 2019) for dimensionality reduction of hand vertices and encode joint rotations as 6D vectors. And then, we import these information as well as joint rotations and hand types into the hand-structure processor. The structure of hand-structure processor consists of two parallel blocks: three stacked layers of linear and ReLU activation (L_r) and two stacked layers of linear and layer normalization (L_n). These streamlined hand vertices and joint locations are then fed into L_r . Concurrently, joint rotations and hand types are transformed via L_n . The outputs from these processes are aggregated to form the Hand Structural Embedding C_{struc} , encapsulating essential geometric and 3D information for precise hand representation.

$$C_{struc} = [L_r(V_h), L_r(J_{2d}), L_n(T_h), L_n(\theta_h)]. \quad (3)$$

Hand appearance embedding. To improve hand visual detail, we extract features $\mathcal{F} \in \mathbb{R}^{n \times 1536}$ from the hand Bounding Box regions using DINOv2 (Oquab et al. 2023). The Hand-Appear processor(HA) uses a linear layer followed by Layer Normalization (Ba, Kiros, and Hinton 2016), culminating in the Hand Appearance Embedding C_{appear} . This process ensures the hand’s visual fidelity and detail are meticulously preserved in our representation.

$$C_{appear} = HA(\mathcal{F}). \quad (4)$$



(I) Qualitative results on DressCode



(II) Qualitative results on VITON-HD

Figure 3: Qualitative comparisons of VTON-HandFit with other methods on public datasets: (I) Dresscode and (II) VITON-HD.

Mask-based regional control. Our method introduces a mask-based regional control to enhance hand detail generation and maintain quality in virtual try-on. Utilizing the hand mask M_h , we modulate Cross-Attention queries, seamlessly integrating Hand Structural Embedding within HandposeNet’s Cross-Attention module. Concurrently, Hand Appearance Embedding is adeptly fused into the TryonNet architecture through mask cross-attention, ensuring precise detail preservation. The mask cross-attention can be represented as:

$$\begin{aligned} Z &= \text{Attention}(Q, K, V, M_h) \\ &= \text{Softmax}\left(\frac{QM_hK^\top}{\sqrt{d}}\right)V, \end{aligned} \quad (5)$$

where Q , K and V are the query, key, and value matrices of the attention operation for hand appearance embedding cross-attention, M_h represents the hand mask.

Hand canny shape constraint. During the training process, \mathcal{L}_{hand} is implemented to refine the clarity and precision of hand edges. Specifically, for a small $R_t < T$, we employ one-step denoising process prior to sampling x_0 for the direct prediction of z_0 from z_t and the model-predicted noise, using Variational Autoencoder for decoder.

$$z_0 = \frac{z_t - \sqrt{1 - \bar{\alpha}_t}\epsilon_\theta}{\sqrt{\bar{\alpha}_t}}, \quad t \leq R_t. \quad (6)$$

Hand regions are extracted from the generated images using bounding box cropping and are processed with the Canny edge detection operator. These regions are then compared to their corresponding areas in the Ground Truth images using Mean Squared Error (MSE) loss. This loss function is specifically designed to sharpen the model’s focus on improving edge details and clarity in the hand regions of the generated images.

$$\mathcal{L}_{hand} = \begin{cases} \frac{1}{N} \sum_{i=1}^N \left(\phi(I_{gen}^{(i)}) - \phi(I_{GT}^{(i)}) \right)^2 & t \leq R_t \\ 0, & t > R_t \end{cases}, \quad (7)$$

where N represents the number of images, $I_{gen}^{(i)}$ denotes the i -th generated image, and $I_{GT}^{(i)}$ denotes the i -th ground truth image. The function $\phi(\cdot)$ applies the Canny edge detection operator to the images.

Experiment

Baselines. To comprehensively evaluate our approach, we selected five state-of-the-art diffusion-based methods in the virtual try-on domain as baselines for comparison: LaDI-VTON (Morelli et al. 2023), StableVTON (Kim et al. 2024), OOTDiffusion (Xu et al. 2024), IDM-VTON (Choi et al. 2024), and CatVTON (Zeng et al. 2024). While these meth-



Figure 4: Qualitative comparisons of VTON-HandFit with other methods on our Handfit-3K dataset. In Handfit-3K, we remark that the hands in the images are occluded, making it difficult to distinguish them directly through masks.

Methods	DressCode						VITON-HD					
	Paired				Unpaired		Paired				Unpaired	
	SSIM \uparrow	LPIPS \downarrow	FID \downarrow	KID \downarrow	FID \downarrow	KID \downarrow	SSIM \uparrow	LPIPS \downarrow	FID \downarrow	KID \downarrow	FID \downarrow	KID \downarrow
LaDI-VTON (2023)	0.9025	0.0719	4.8636	1.5580	6.8421	2.3345	0.8763	0.0911	6.6044	1.0672	9.4095	1.6866
StableVTON (2024)	-	-	-	-	-	-	0.8665	0.0835	6.8581	1.2553	9.5868	1.4508
IDM-VTON (2024)	0.9228	0.0478	3.8001	1.2012	5.6159	1.5536	0.8806	0.0789	6.3381	1.3224	9.6114	1.6387
OOTDiffusion (2024)	0.8975	0.0725	3.9497	0.7198	6.7019	1.8630	0.8513	0.0964	6.5186	0.8961	9.6733	1.2061
CatVTON (2024)	0.9011	0.0705	3.2755	0.6696	5.4220	1.5490	0.8694	0.0970	6.1394	0.9639	9.1434	1.2666
VTON-HandFit (Ours)	0.9404	0.0444	2.8666	0.8009	5.2314	1.0189	0.8850	0.0730	5.9564	0.9699	8.8178	0.9951

Table 1: Quantitative results on VITON-HD and DressCode datasets. We compare the metrics under both paired (model’s clothing is the same as the given cloth image) and unpaired settings (model’s clothing differs) with other methods.

Methods	Paired							Unpaired				
	SSIM \uparrow	LPIPS \downarrow	FID \downarrow	KID \downarrow	MPJPE \downarrow	FID-H \downarrow	KID-H \downarrow	FID \downarrow	KID \downarrow	MPJPE \downarrow	FID-H \downarrow	KID-H \downarrow
LaDI-VTON (2023)	0.8597	0.1480	12.8430	4.4112	107.6315	23.0199	17.4558	16.2506	7.0065	111.1547	21.1371	14.1960
StableVTON (2024)	0.8772	0.1022	11.3675	4.1360	54.7586	22.7470	16.699	14.0446	5.1966	57.3334	22.8099	16.3022
IDM-VTON (2024)	0.8816	0.0935	7.7159	2.1287	48.6378	11.5403	3.9727	11.2960	3.4638	57.3447	12.7721	4.4315
OOTDiffusion (2024)	0.8554	0.1184	8.7104	2.1363	83.9655	12.1984	3.6653	13.1969	4.4839	86.1678	13.8011	4.4479
CatVTON (2024)	0.8761	0.1123	10.6966	4.2581	60.6608	13.1264	4.8723	15.7081	6.9544	63.2245	15.5603	5.6134
VTON-HandFit (Ours)	0.8827	0.0819	5.6027	0.4932	25.1376	7.0574	1.2474	10.9786	3.3248	26.6892	9.0003	2.5362

Table 2: Quantitative results on Handfit-3K dataset in the paired and unpaired settings.

ods have made substantial contributions to the virtual try-on field, they exhibit certain limitations in handling hand occlusion issues, which motivated us to propose VTON-HandFit.

Dataset. Our experiments utilize two publicly virtual try-on datasets: VITON-HD (Choi et al. 2021) and DressCode (Morelli et al. 2022). The VITON-HD dataset consists of 13,679 image pairs, divided into 11,647 for training and 2,032 for testing, featuring front-facing upper-body portraits paired with garments at a resolution of 1024 \times 768. The DressCode dataset, larger and more varied, contains 48,392 training pairs and 5,400 testing pairs, including full-body portraits and a range of garments (upper-body, lower-body, and dresses) at the same resolution. To enhance our evaluation of the model’s capability to address hand occlusion challenges, we build *Handfit-3K* test with 3,620 images sorted from 26,000 images collected in online retail sites.

Evaluation metrics. Following previous works (Morelli et al. 2023; Kim et al. 2024), we adopt both paired and unpaired evaluation settings. In the paired setting, the quality of the generated images is assessed using Structural Similarity (SSIM) (Wang et al. 2004), Learned Perceptual Image Patch Similarity (LPIPS) (Zhang et al. 2018), Frechet Inception

Distance (FID) (Heusel et al. 2017), and Kernel Inception Distance (KID) (Binkowski et al. 2018). For the unpaired setting, we employ FID and KID for comparison. Hand generation quality is assessed using FID-H and KID-H for the hand region. Additionally, we use 2D Mean Per Joint Position Error (MPJPE) (Ionescu et al. 2013) to evaluate hand joint position accuracy.

Implementation details. Our model is developed using the pre-trained StableDiffusion v1.5 (Rombach et al. 2022). Detailed body dynamics and structural information are captured using DWpose (Yang et al. 2023c) for pose estimation, Detectron2 (Wu et al. 2019) for Densepose segmentation, and HaMeR for detailed hand depth maps and parameters. We use VITON-HD and DressCode datasets for training. Our training strategy is implemented in two phases. In the first phase, we train the Hand-Pose Aggregation Net and Hand-feature Disentanglement Embedding modules while freezing the other components. In the second phase, we refine the TryonNet and GarmentNet. All models are trained uniformly with a batch size of 32, employing the AdamW (Loshchilov and Hutter 2017) optimizer at a learning rate of 5e-5. Training is conducted on 8 NVIDIA V100 GPUs.



Figure 5: Qualitative comparisons in real-world scenarios.

Results on Public Dataset

Qualitative results. Fig. 3 shows visual comparisons of the VTON-HD and DressCode datasets between VTON-HandFit and other methods. In previous methods, original hand regions are often reused, leading to artifacts such as blue outlines around the hands when garment colors significantly differ (third row). In contrast, our model effectively eliminates these residual backgrounds and preserves natural hand poses, enhancing visual fidelity and pose accuracy.

Quantitative results. Tab. 1 presents the quantitative comparisons of VTON-HandFit against other state-of-the-art methods on VTON-HD and DressCode datasets. By enhancing pose accuracy and the fidelity of hand gestures, our approach achieves markedly improved synthesized image quality. Moreover, VTON-HandFit outperforms in FID and KID scores across both datasets in unpaired settings, underscoring the importance of precise hand pose representation for enhancing image quality in practical applications.

Results on Handfit-3K Dataset

Qualitative results. Fig. 4 presents a qualitative comparison between VTON-HandFit and other diffusion-based methods. Our method outperforms in preserving detailed garment attributes and achieving natural hand poses. The images generated by VTON-HandFit demonstrate superior consistency in texture, pattern, and fit relative to baseline methods. Furthermore, the hand poses in our images are more consistent with the original.

Quantitative results. Tab. 2 consolidates the performance of VTON-HandFit against contemporary methods on the Handfit-3K dataset. VTON-HandFit excels in both paired and unpaired settings, showcasing marked advancements in MPJPE, FID-H, and KID-H metrics. This evidences its capability to generate visually compelling images with precise hand pose representation and detailed hand regions. The model’s robustness is further affirmed in the unpaired setting, where it consistently leads across all metrics, reinforcing its practical applicability in virtual try-on scenarios with a focus on hand detail fidelity.

Results of real-world scenarios. To verify the performance of our VTON-HandFit in real-world scenarios, we collect some cases in the wild as shown in Fig. 5.

Ablation Study

Effectiveness of each component. We perform an ablation study to evaluate the contributions of the Hand-Pose Aggregation Net, Hand Structural Embedding C_{struct} , and Hand Appearance Embedding C_{appear} . To facilitate

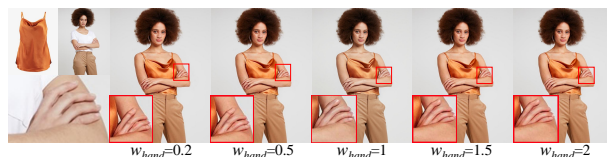


Figure 6: Effect of varying control strength w_{hand} on hand shape and texture. As w_{hand} increases from 0.2 to 2, the hand shape and pose better match the depth map, but higher control strengths lead to a loss of hand wrinkles and textures.



Figure 7: Qualitative comparisons of VTON-HandFit with variants on VTON-HD dataset.

Methods	SSIM \uparrow	LPIS \downarrow	FID \downarrow	KID \downarrow
Baseline	0.8619	0.0923	6.9549	1.2651
Baseline+HPA(Densepose)	0.8660	0.0876	6.8924	1.1254
Baseline+HPA	0.8738	0.0812	6.3390	0.9502
Baseline+HPA+ C_{struct}	0.8784	0.0787	6.2225	1.1186
Baseline+HPA+ $C_{struct} + C_{appear}$	0.8787	0.0792	6.0515	1.0084
VTON-HandFit	0.8850	0.0730	5.9564	0.9699

Table 3: Comparison of different variants on VTON-HD dataset.

a clear comparison, we introduce several model variants to ascertain the effectiveness of each component. The ‘Baseline’ model excludes all specialized components. The ‘Baseline+HPA (Densepose)’ variant incorporates only Densepose for pose control. ‘Baseline+HPA’ utilizes Densepose, Depth, and DWpose for pose control. ‘Baseline+HPA+ C_{struct} ’ excludes the appearance embedding. Lastly, ‘Baseline+HPA+ $C_{struct}+C_{appear}$ ’ incorporates all components. These variants do not include hand-canny constraint loss. Tab. 3 presents a quantitative comparison of our ablation experiments, highlighting the impact of adding different components on the image generation quality. Fig. 7 offers a qualitative analysis, showing the necessity of pose guidance for accurate arm pose replication in the model. By incorporating stronger hand structure and visual guidance, the generation of hands is significantly improved. **Study of adjustable hand weight.** We investigate the influence of varying the control strength of depth maps for different hands on the generated images. Fig. 6 shows that under complex hand poses, the model may produce deformed hand postures. By increasing the control strength of the depth maps, more accurate and complete hand formations are achieved.

Conclusion

We propose VTON-HandFit, a novel model designed for addressing hand occlusion in virtual try-on scenario. Specifically, we have developed a Handpose Aggregation Net by explicitly and adaptively encoding global hand and pose priors using the ControlNet-based structure. To fully exploit the hand-related structure and appearance information, we propose the Hand-feature Disentanglement Embedding module, which explicitly separates the hand priors into hand structure-parametric and visual-appearance features. Lastly, we have customized a hand-canny constraint loss to enhance

the learning of structural edge knowledge from the hand template of the model image. Our approach has been extensively evaluated qualitatively and quantitatively, demonstrating its superiority over state-of-the-art virtual try-on models, particularly in cases involving hand pose occlusion. These results pave the way for more complex virtual try-on applications toward real-world scenarios.

References

- Ba, J. L.; Kiros, J. R.; and Hinton, G. E. 2016. Layer normalization. *arXiv preprint arXiv:1607.06450*.
- Bhunia, A. K.; Khan, S.; Cholakkal, H.; Anwer, R. M.; Laaksonen, J.; Shah, M.; and Khan, F. S. 2023. Person image synthesis via denoising diffusion model. In *Proceedings of the IEEE/CVF Conference on Computer Vision and Pattern Recognition*, 5968–5976.
- Bińkowski, M.; Sutherland, D. J.; Arbel, M.; and Gretton, A. 2018. Demystifying mmd gans. *arXiv preprint arXiv:1801.01401*.
- Cao, S.; Chai, W.; Hao, S.; Zhang, Y.; Chen, H.; and Wang, G. 2023. Diffashion: Reference-based fashion design with structure-aware transfer by diffusion models. *IEEE Transactions on Multimedia*.
- Chen, M.; Chen, X.; Zhai, Z.; Ju, C.; Hong, X.; Lan, J.; and Xiao, S. 2024. Wear-any-way: Manipulable virtual try-on via sparse correspondence alignment. *arXiv preprint arXiv:2403.12965*.
- Choi, S.; Park, S.; Lee, M.; and Choo, J. 2021. Viton-hd: High-resolution virtual try-on via misalignment-aware normalization. In *Proceedings of the IEEE/CVF conference on computer vision and pattern recognition*, 14131–14140.
- Choi, Y.; Kwak, S.; Lee, K.; Choi, H.; and Shin, J. 2024. Improving diffusion models for virtual try-on. *ECCV*.
- Davide, M.; Matteo, F.; Marcella, C.; Federico, L.; Fabio, C.; and Rita, C. 2022. Dress code: High-resolution multi-category virtual try-on. In *Proceedings of the IEEE/CVF Conference on Computer Vision and Pattern Recognition*.
- Dong, H.; Liang, X.; Shen, X.; Wang, B.; Lai, H.; Zhu, J.; Hu, Z.; and Yin, J. 2019. Towards multi-pose guided virtual try-on network. In *Proceedings of the IEEE/CVF international conference on computer vision*, 9026–9035.
- Ge, C.; Song, Y.; Ge, Y.; Yang, H.; Liu, W.; and Luo, P. 2021a. Disentangled cycle consistency for highly-realistic virtual try-on. In *Proceedings of the IEEE/CVF conference on computer vision and pattern recognition*, 16928–16937.
- Ge, Y.; Song, Y.; Zhang, R.; Ge, C.; Liu, W.; and Luo, P. 2021b. Parser-free virtual try-on via distilling appearance flows. In *Proceedings of the IEEE/CVF conference on computer vision and pattern recognition*, 8485–8493.
- Goodfellow, I.; Pouget-Abadie, J.; Mirza, M.; Xu, B.; Warde-Farley, D.; Ozair, S.; Courville, A.; and Bengio, Y. 2020. Generative adversarial networks. *Communications of the ACM*, 63(11): 139–144.
- Gou, J.; Sun, S.; Zhang, J.; Si, J.; Qian, C.; and Zhang, L. 2023. Taming the power of diffusion models for high-quality virtual try-on with appearance flow. In *Proceedings of the 31st ACM International Conference on Multimedia*, 7599–7607.
- Han, X.; Hu, X.; Huang, W.; and Scott, M. R. 2019. Cloth-flow: A flow-based model for clothed person generation. In *Proceedings of the IEEE/CVF international conference on computer vision*, 10471–10480.
- Han, X.; Wu, Z.; Wu, Z.; Yu, R.; and Davis, L. S. 2018. Viton: An image-based virtual try-on network. In *Proceedings of the IEEE conference on computer vision and pattern recognition*, 7543–7552.
- He, S.; Song, Y.-Z.; and Xiang, T. 2022. Style-based global appearance flow for virtual try-on. In *Proceedings of the IEEE/CVF Conference on Computer Vision and Pattern Recognition*, 3470–3479.
- Heusel, M.; Ramsauer, H.; Unterthiner, T.; Nessler, B.; and Hochreiter, S. 2017. Gans trained by a two time-scale update rule converge to a local nash equilibrium. *Advances in neural information processing systems*, 30.
- Hu, X.; Peng, X.; Luo, D.; Ji, X.; Peng, J.; Jiang, Z.; Zhang, J.; Jin, T.; Wang, C.; and Ji, R. 2024. DiffuMatting: Synthesizing Arbitrary Objects with Matting-level Annotation. *arXiv preprint arXiv:2403.06168*.
- Ionescu, C.; Papava, D.; Olaru, V.; and Sminchisescu, C. 2013. Human3.6m: Large scale datasets and predictive methods for 3d human sensing in natural environments. *IEEE transactions on pattern analysis and machine intelligence*, 36(7): 1325–1339.
- Issenhuth, T.; Mary, J.; and Calauzenes, C. 2020. Do not mask what you do not need to mask: a parser-free virtual try-on. In *Computer Vision–ECCV 2020: 16th European Conference, Glasgow, UK, August 23–28, 2020, Proceedings, Part XX 16*, 619–635. Springer.
- Karras, J.; Holynski, A.; Wang, T.-C.; and Kemelmacher-Shlizerman, I. 2023. Dreampose: Fashion image-to-video synthesis via stable diffusion. In *2023 IEEE/CVF International Conference on Computer Vision (ICCV)*, 22623–22633. IEEE.
- Kawar, B.; Zada, S.; Lang, O.; Tov, O.; Chang, H.; Dekel, T.; Mosseri, I.; and Irani, M. 2023. Imagic: Text-based real image editing with diffusion models. In *Proceedings of the IEEE/CVF Conference on Computer Vision and Pattern Recognition*, 6007–6017.
- Kim, J.; Gu, G.; Park, M.; Park, S.; and Choo, J. 2024. Stableviton: Learning semantic correspondence with latent diffusion model for virtual try-on. In *Proceedings of the IEEE/CVF Conference on Computer Vision and Pattern Recognition*, 8176–8185.
- Kumari, N.; Zhang, B.; Zhang, R.; Shechtman, E.; and Zhu, J.-Y. 2023. Multi-concept customization of text-to-image diffusion. In *Proceedings of the IEEE/CVF Conference on Computer Vision and Pattern Recognition*, 1931–1941.
- Lee, S.; Gu, G.; Park, S.; Choi, S.; and Choo, J. 2022. High-resolution virtual try-on with misalignment and occlusion-handled conditions. In *European Conference on Computer Vision*, 204–219. Springer.

- Li, Y.; Zhou, H.; Shang, W.; Lin, R.; Chen, X.; and Ni, B. 2024. AnyFit: Controllable Virtual Try-on for Any Combination of Attire Across Any Scenario. *arXiv preprint arXiv:2405.18172*.
- Loshchilov, I.; and Hutter, F. 2017. Decoupled weight decay regularization. *arXiv preprint arXiv:1711.05101*.
- Lu, W.; Xu, Y.; Zhang, J.; Wang, C.; and Tao, D. 2023. Handrefiner: Refining malformed hands in generated images by diffusion-based conditional inpainting. In *ACM Multimedia 2024*.
- Men, Y.; Mao, Y.; Jiang, Y.; Ma, W.-Y.; and Lian, Z. 2020. Controllable person image synthesis with attribute-decomposed gan. In *Proceedings of the IEEE/CVF conference on computer vision and pattern recognition*, 5084–5093.
- Morelli, D.; Baldrati, A.; Cartella, G.; Cornia, M.; Bertini, M.; and Cucchiara, R. 2023. Ladi-vton: Latent diffusion textual-inversion enhanced virtual try-on. In *Proceedings of the 31st ACM International Conference on Multimedia*, 8580–8589.
- Morelli, D.; Fincato, M.; Cornia, M.; Landi, F.; Cesari, F.; and Cucchiara, R. 2022. Dress code: High-resolution multi-category virtual try-on. In *Proceedings of the IEEE/CVF conference on computer vision and pattern recognition*, 2231–2235.
- Mou, C.; Wang, X.; Xie, L.; Wu, Y.; Zhang, J.; Qi, Z.; and Shan, Y. 2024. T2i-adapter: Learning adapters to dig out more controllable ability for text-to-image diffusion models. In *Proceedings of the AAAI Conference on Artificial Intelligence*, volume 38, 4296–4304.
- Oquab, M.; Darcet, T.; Moutakanni, T.; Vo, H.; Szafraniec, M.; Khalidov, V.; Fernandez, P.; Haziza, D.; Massa, F.; El-Nouby, A.; et al. 2023. Dinov2: Learning robust visual features without supervision. *arXiv preprint arXiv:2304.07193*.
- Pavlakos, G.; Shan, D.; Radosavovic, I.; Kanazawa, A.; Fouhey, D.; and Malik, J. 2024. Reconstructing hands in 3d with transformers. In *Proceedings of the IEEE/CVF Conference on Computer Vision and Pattern Recognition*, 9826–9836.
- Podell, D.; English, Z.; Lacey, K.; Blattmann, A.; Dockhorn, T.; Müller, J.; Penna, J.; and Rombach, R. 2023. Sdxl: Improving latent diffusion models for high-resolution image synthesis. *arXiv preprint arXiv:2307.01952*.
- Prokudin, S.; Lassner, C.; and Romero, J. 2019. Efficient learning on point clouds with basis point sets. In *Proceedings of the IEEE/CVF international conference on computer vision*, 4332–4341.
- Rombach, R.; Blattmann, A.; Lorenz, D.; Esser, P.; and Ommer, B. 2022. High-resolution image synthesis with latent diffusion models. In *Proceedings of the IEEE/CVF conference on computer vision and pattern recognition*, 10684–10695.
- Ruiz, N.; Li, Y.; Jampani, V.; Pritch, Y.; Rubinstein, M.; and Aberman, K. 2023. Dreambooth: Fine tuning text-to-image diffusion models for subject-driven generation. In *Proceedings of the IEEE/CVF conference on computer vision and pattern recognition*, 22500–22510.
- Saharia, C.; Chan, W.; Chang, H.; Lee, C.; Ho, J.; Salimans, T.; Fleet, D.; and Norouzi, M. 2022. Palette: Image-to-image diffusion models. In *ACM SIGGRAPH 2022 conference proceedings*, 1–10.
- Samuel, D.; Ben-Ari, R.; Raviv, S.; Darshan, N.; and Chechik, G. 2024. Generating images of rare concepts using pre-trained diffusion models. In *Proceedings of the AAAI Conference on Artificial Intelligence*, volume 38, 4695–4703.
- Sun, K.; Cao, J.; Wang, Q.; Tian, L.; Zhang, X.; Zhuo, L.; Zhang, B.; Bo, L.; Zhou, W.; Zhang, W.; et al. 2024. OutfitAnyone: Ultra-high Quality Virtual Try-On for Any Clothing and Any Person. *arXiv preprint arXiv:2407.16224*.
- Wang, C.; Liu, P.; Zhou, M.; Zeng, M.; Li, X.; Ge, T.; et al. 2024. RHandDS: Refining Malformed Hands for Generated Images with Decoupled Structure and Style Guidance. *arXiv preprint arXiv:2404.13984*.
- Wang, Z.; Bovik, A. C.; Sheikh, H. R.; and Simoncelli, E. P. 2004. Image quality assessment: from error visibility to structural similarity. *IEEE transactions on image processing*, 13(4): 600–612.
- Wu, Y.; Kirillov, A.; Massa, F.; Lo, W.-Y.; and Girshick, R. 2019. Detectron2. <https://github.com/facebookresearch/detectron2>.
- Xie, Z.; Huang, Z.; Dong, X.; Zhao, F.; Dong, H.; Zhang, X.; Zhu, F.; and Liang, X. 2023. Gp-vton: Towards general purpose virtual try-on via collaborative local-flow global-parsing learning. In *Proceedings of the IEEE/CVF Conference on Computer Vision and Pattern Recognition*, 23550–23559.
- Xu, Y.; Gu, T.; Chen, W.; and Chen, C. 2024. Ootdiffusion: Outfitting fusion based latent diffusion for controllable virtual try-on. *arXiv preprint arXiv:2403.01779*.
- Yang, B.; Gu, S.; Zhang, B.; Zhang, T.; Chen, X.; Sun, X.; Chen, D.; and Wen, F. 2023a. Paint by example: Exemplar-based image editing with diffusion models. In *Proceedings of the IEEE/CVF Conference on Computer Vision and Pattern Recognition*, 18381–18391.
- Yang, H.; Zhang, R.; Guo, X.; Liu, W.; Zuo, W.; and Luo, P. 2020. Towards photo-realistic virtual try-on by adaptively generating-preserving image content. In *Proceedings of the IEEE/CVF conference on computer vision and pattern recognition*, 7850–7859.
- Yang, Z.; Chen, J.; Shi, Y.; Li, H.; Chen, T.; and Lin, L. 2023b. OccluMix: Towards de-occlusion virtual try-on by semantically-guided mixup. *IEEE Transactions on Multimedia*, 25: 1477–1488.
- Yang, Z.; Zeng, A.; Yuan, C.; and Li, Y. 2023c. Effective whole-body pose estimation with two-stages distillation. In *Proceedings of the IEEE/CVF International Conference on Computer Vision*, 4210–4220.
- Ye, H.; Zhang, J.; Liu, S.; Han, X.; and Yang, W. 2023. Ip-adapter: Text compatible image prompt adapter for text-to-image diffusion models. *arXiv preprint arXiv:2308.06721*.
- Zeng, J.; Song, D.; Nie, W.; Tian, H.; Wang, T.; and Liu, A.-A. 2024. CAT-DM: Controllable Accelerated Virtual Try-on with Diffusion Model. In *Proceedings of the IEEE/CVF*

Conference on Computer Vision and Pattern Recognition, 8372–8382.

Zhang, H.; Li, F.; Liu, S.; Zhang, L.; Su, H.; Zhu, J.; Ni, L. M.; and Shum, H.-Y. 2023. Dino: Detr with improved de-noising anchor boxes for end-to-end object detection. *ICLR*.

Zhang, L.; Rao, A.; and Agrawala, M. 2023. Adding conditional control to text-to-image diffusion models. In *Proceedings of the IEEE/CVF International Conference on Computer Vision*, 3836–3847.

Zhang, R.; Isola, P.; Efros, A. A.; Shechtman, E.; and Wang, O. 2018. The unreasonable effectiveness of deep features as a perceptual metric. In *Proceedings of the IEEE conference on computer vision and pattern recognition*, 586–595.

Zhang, X.; Lin, E.; Li, X.; Luo, Y.; Kampffmeyer, M.; Dong, X.; and Liang, X. 2024. MMTryon: Multi-Modal Multi-Reference Control for High-Quality Fashion Generation. *arXiv preprint arXiv:2405.00448*.

Zhao, S.; Chen, D.; Chen, Y.-C.; Bao, J.; Hao, S.; Yuan, L.; and Wong, K.-Y. K. 2024. Uni-controlnet: All-in-one control to text-to-image diffusion models. *Advances in Neural Information Processing Systems*, 36.

Zhu, L.; Yang, D.; Zhu, T.; Reda, F.; Chan, W.; Saharia, C.; Norouzi, M.; and Kemelmacher-Shlizerman, I. 2023. Tryondiffusion: A tale of two unets. In *Proceedings of the IEEE/CVF Conference on Computer Vision and Pattern Recognition*, 4606–4615.